Solar Phys (2017) 292:95
DOI 10.1007/s11207-017-1119-y

# Shannon Entropy-Based Prediction of Solar Cycle 25

**Bharati Kakad[1] · Amar Kakad[1] · Durbha Sai Ramesh[1]**

Received: 6 March 2017 / Accepted: 1 June 2017 / Published online: 12 July 2017


**Abstract** A new model is proposed to forecast the peak sunspot activity of the upcoming solar cycle (SC) using Shannon entropy estimates related to the declining phase of the preceding SC. Daily and monthly smoothed international sunspot numbers are used in the present study. The Shannon entropy is the measure of inherent randomness in the SC and is found to vary with the phase of an SC as it progresses. In this model each SC with length $T_{cy}$ is divided into five equal parts of duration $T_{cy}/5$. Each part is considered as one phase, and they are sequentially termed P1, P2, P3, P4, and P5. The Shannon entropy estimates for each of these five phases are obtained for the $n$th SC starting from $n = 10-23$. We find that the Shannon entropy during the ending phase (P5) of the $n$th SC can be efficiently used to predict the peak smoothed sunspot number of the $(n + 1)$th SC, *i.e.* $S_{max}^{n+1}$. The prediction equation derived in this study has a good correlation coefficient of 0.94. A noticeable decrease in entropy from 4.66 to 3.89 is encountered during P5 of SCs 22 to 23. The entropy value for P5 of the present SC 24 is not available as it has not yet ceased. However, if we assume that the fall in entropy continues for SC 24 at the same rate as that for SC 23, then we predict the peak smoothed sunspot number of $63\pm11.3$ for SC 25. It is suggested that the upcoming SC 25 will be significantly weaker and comparable to the solar activity observed during the Dalton minimum in the past.

**Keywords** Solar cycle · Sunspots · Models

✉ B. Kakad
bkakad9@gmail.com

A. Kakad
amar.kakad@gmail.com

D.S. Ramesh
dsramesh@iigs.iigm.res.in

[1] Indian Institute of Geomagnetism, Plot 5, Sector 18, New Panel (W), Navi Mumbai, 410218, Maharashtra, India

## 1. Introduction

Prediction of an upcoming solar cycle has always been a topic of great interest to space scientists and technologists. As the Sun is the source of energy for our planet, the variability in the solar energy emitted in the form of radiation and highly energetic particles affects our life and near-Earth environment, including space-based communication systems and technology (McComas *et al.*, 2008; Emmert, Lean, and Picone, 2010; de Toma *et al.*, 2010; Ermolli *et al.*, 2013; Solomon, Qian, and Burns, 2013; Hajra *et al.*, 2014; Hao *et al.*, 2014). It would not be an exaggeration to call the Sun the master controller of our space weather. Solar cycles (SCs) with extremely low solar activity for prolonged periods, such as the Maunder minimum and Dalton minimum, have been observed in the past. Several studies using proxies for solar activity have suggested the presence of grand minima in the SC (Usoskin, Solanki, and Kovaltsov, 2007, 2011). Curiosity about future solar activity resulted in a number of studies proposing various models to forecast peak solar activity. Some of the prediction models were based on data that used various proxies of solar activity, *viz* F10.7 cm solar flux, sunspot number, and *aa* index (Ohl, 1966; Feynman, 1982; Wilson, 1990; Thompson, 1993; Hathaway and Wilson, 2006; Kane, 2007; Pesnell, 2014). Other models were based on dynamo theory (Dikpati and Charbonneau, 1999; Dikpati, De Toma, and Gilman, 2006; Dikpati and Gilman, 2008). In addition to this, the strength of the solar polar magnetic field was also used as one of the indicators to forecast the level of an upcoming solar cycle (Svalgaard, Cliver, and Kamide, 2005; Muñoz-Jaramillo *et al.*, 2013; Svalgaard and Kamide, 2012). The forecast from the above-mentioned methods are either available before or close to the solar minimum or after initiation of a SC.

Although many prediction models are available today, their usage depends upon the reliability of their forecast. For instance, Clilverd *et al.* (2006) predicted the smoothed sunspot number (SSN) to be 42 for SC 24. Based on the solar polar magnetic field, Svalgaard, Cliver, and Kamide (2005) forecast the SSN to be 75, and Pishkalo (2014) gave a prediction of SSN $90\pm12$ for SC 24. Kakad (2011) suggested that the SSN for SC 24 could be 74. Later, an expert panel of NASA predicted a peak SSN of 101 late in 2013 for SC 24 (https://solarscience.msfc.nasa.gov/predict.shtml). Gkana and Zachilas (2015) used monthly sunspot numbers and gave a forecast of 92.4 for the peak SSN of SC 24, which is in close agreement with the observed SSN. Comparison of predictions for SC 24 using fifty different available methods were presented by Pesnell (2008, 2016). Now we know that the current SC 24 reached a peak of 102.3 in monthly and 81.9 in monthly smoothed sunspot numbers close to February 2014 and April 2014, respectively. This suggests that the forecasts by some of the models were close to the observed SSN for SC 24, whereas other model predictions either underestimated or overestimated the peak SSN for SC 24. Thus, it is essential to develop precise prediction models to forecast solar activity with the least errors.

Earlier studies demonstrated that sunspot time series possess chaotic behavior (Mundt, Maguire, and Chase, 1991; Price, Prichard, and Hogenson, 1992; Zachilas and Gkana, 2015). In such chaotic systems, prediction of the present state is difficult because of the very high dependence on the initial conditions. Application of a technique based on the Shannon entropy, which represents the inherent randomness in the system, could be a good candidate to understand such systems. In the present study, we develop a new model based on the Shannon entropy to forecast the peak SSN of an upcoming SC. This model uses the sunspot observations from SCs $10-23$. The method adopted to construct the model is described in Section 2. The results are discussed and the proposed model equation is validated in Section 3. Conclusions from the present study and the forecast for SC 25 are given in Section 4.

## 2. Method

In this study, we use the daily and monthly smoothed international sunspot numbers Version 1 dataset, which is available at http://www.sidc.be/silso/. Before we proceed with the model development, the characteristics of each SC, namely, ascent time ($T_a$), descent time ($T_d$), length ($T_{cy}$), maximum sunspot number ($S_{max}$), and minimum sunspot number ($S_{min}$) are estimated using the monthly smoothed sunspot number (SSN) data. In order to obtain these characteristics, it is important to establish the start time ($t_s$), peak ($t_p$), and end ($t_e$) for each SC. The start and peak times of the $n$th SC are associated with the occurrence of the minimum and maximum in the SSN for the $n$th SC, respectively. The end time for the $n$th SC is the same as the start time for the $(n+1)$th SC (*i.e.* $t_e^n = t_s^{n+1}$). The occurrence of the minimum and maximum for a given SC is obtained by taking the mathematical minimum and maximum in the monthly SSN. If the same value of minimum/maximum is encountered in the monthly SSN more than once, then its first occurrence is treated as the time of minimum/maximum for the corresponding SC. Thus, the characteristics for the $n$th SC are given by the ascent time $T_a^n = t_p^n - t_s^n$, descent time $T_d^n = t_e^n - t_p^n$, and length $T_{cy}^n = T_a^n + T_d^n$. The monthly SSN at the time of $t_p^n$ and $t_s^n$ are represented by $S_{max}^n$ and $S_{min,}^n$ respectively, for each $n$th SC. We present these characteristics for SCs 1 – 24 in Table 1. Details of the estimated characteristics of each SC using other methods can be found in the review article by Hathaway (2010). The SC characteristics obtained from three different methods were compared by Kakad (2011), and their study suggested very small deviation among them. Thus, we chose to use the method based on mathematical minimum/maximum in the monthly SSN to derive the SC characteristics.

The second step is to obtain the estimates of the Shannon entropy from the daily sunspot numbers. We apply the technique of the Shannon entropy to SCs 10 – 24 as the daily sunspot number data do not have major data losses during this period. The concept of the Shannon entropy is well known and was introduced by Shannon (1948) in the information theory seventy years ago. However, its application, particularly to space weather, climate, and Earth-related studies has certainly increased during recent decades. It is used as an important tool to understand the link between various phenomena involving cause-and-effect relationships (Materassi, Wernik, and Yordanova, 2007; De Michelis *et al.*, 2011; Bapanayya *et al.*, 2011; Das Sharma *et al.*, 2012; Zhao and Qin, 2013; Vichare, Bhaskar, and Ramesh, 2016). Recently, Kakad, Kakad, and Ramesh (2015) computed the Shannon entropy associated with each SC and used it to predict the descent time of the forthcoming SC. In the present study, we have explored the possibility of using information of the Shannon entropy from preceding SCs to develop a forecasting model for the peak activity of the upcoming SC.

The Shannon entropy is a measure of randomness present in a system, which is described by the given data series. When computing the Shannon entropy from daily sunspot numbers, one has to obtain the information on variations present in the original time series. This is accomplished by applying a moving average filter to the original data (Carbone, Castelli, and Stanley, 2004). We denote these variations by $\Delta S$, and for each $j$th day it is estimated using

$$\Delta S(j) = S(j) - \frac{1}{L} \sum_{k=j-(L-1)/2}^{k=j+(L-1)/2} S(k), \tag{1}$$

where $S(j)$ is the daily sunspot number for the $j$th day and $L$ is the size of the smoothing window. For each $j$th day, we estimate the average value of the sunspot number over a length of window $[L]$ centered on that $j$th day. We then remove this mean from the corresponding

**Table 1** Solar cycle characteristics like start time ($t_s$), peak time ($t_p$), end time ($t_e$), ascent time ($T_a$), descent time ($T_d$), length of SC ($T_{cy}$), peak sunspot number ($S_{max}$), and minimum sunspot number ($S_{min}$) for SCs 1 – 24. Estimated value of entropy for Phase 5 of SC 24 is marked in bold case. The prediction of peak sunspot number obtained using the proposed prediction equation and the absolute error in the predictions for SCs 1 – 24 are given in the last two columns. All times are in years.

| SCN | Start time ($t_s$) | Peak time ($t_p$) | End time ($t_e$) | Ascent time ($T_a$) | Descent time ($T_d$) | Length ($T_{cy}$) | $S_{max}$ (Observed) | $S_{min}$ | $E_{P5}$ | $S_{max}$ (Predicted) | $\lvert\zeta_{error}\rvert$ |
|---|---|---|---|---|---|---|---|---|---|---|---|
| 1 | 1755.13 | 1766.38 | 1761.46 | 6.33 | 4.92 | 11.25 | 86.50 | 8.40 | – | – | – |
| 2 | 1766.38 | 1775.46 | 1769.71 | 3.33 | 5.75 | 9.08 | 115.80 | 11.10 | – | – | – |
| 3 | 1775.46 | 1784.71 | 1778.38 | 2.92 | 6.33 | 9.25 | 158.50 | 7.20 | – | – | – |
| 4 | 1784.71 | 1798.29 | 1788.13 | 3.42 | 10.17 | 13.58 | 141.20 | 9.50 | – | – | – |
| 5 | 1798.29 | 1810.13 | 1805.13 | 6.83 | 5.00 | 11.83 | 49.20 | 3.20 | – | – | – |
| 6 | 1810.13 | 1823.21 | 1816.38 | 6.25 | 6.83 | 13.08 | 48.70 | 0.00 | – | – | – |
| 7 | 1823.21 | 1833.88 | 1829.88 | 6.67 | 4.00 | 10.67 | 71.50 | 0.10 | – | – | – |
| 8 | 1833.88 | 1843.54 | 1837.21 | 3.33 | 6.33 | 9.67 | 146.90 | 7.30 | – | – | – |
| 9 | 1843.54 | 1855.96 | 1848.13 | 4.58 | 7.83 | 12.42 | 131.90 | 10.60 | – | – | – |
| 10 | 1855.96 | 1867.21 | 1860.13 | 4.17 | 7.08 | 11.25 | 98.00 | 3.20 | 5.09 | – | – |
| 11 | 1867.21 | 1878.96 | 1870.63 | 3.42 | 8.33 | 11.75 | 140.30 | 5.20 | 4.07 | 125.27 | 15.03 |
| 12 | 1878.96 | 1890.13 | 1883.96 | 5.00 | 6.17 | 11.17 | 74.60 | 2.20 | 3.94 | 95.28 | 20.68 |
| 13 | 1890.13 | 1902.04 | 1894.04 | 3.92 | 8.00 | 11.92 | 87.90 | 5.00 | 3.98 | 85.40 | 2.50 |
| 14 | 1902.04 | 1913.46 | 1906.13 | 4.08 | 7.33 | 11.42 | 64.20 | 2.70 | 3.26 | 60.16 | 4.04 |
| 15 | 1913.46 | 1923.54 | 1917.63 | 4.17 | 5.92 | 10.08 | 105.40 | 1.50 | 4.59 | 103.18 | 2.22 |
| 16 | 1923.54 | 1933.71 | 1928.29 | 4.75 | 5.42 | 10.17 | 78.10 | 5.60 | 4.25 | 81.35 | 3.25 |
| 17 | 1933.71 | 1944.13 | 1937.29 | 3.58 | 6.83 | 10.42 | 119.20 | 3.50 | 4.91 | 93.71 | 25.49 |
| 18 | 1944.13 | 1954.29 | 1947.38 | 3.25 | 6.92 | 10.17 | 151.80 | 7.70 | 4.67 | 176.27 | 24.47 |
| 19 | 1954.29 | 1964.79 | 1958.21 | 3.92 | 6.58 | 10.50 | 201.30 | 3.40 | 4.90 | 188.32 | 12.98 |
| 20 | 1964.79 | 1976.21 | 1968.88 | 4.08 | 7.33 | 11.42 | 110.60 | 9.60 | 4.86 | 118.37 | 7.77 |
| 21 | 1976.21 | 1986.71 | 1979.96 | 3.75 | 6.75 | 10.50 | 164.50 | 12.20 | 4.59 | 156.16 | 8.34 |
| 22 | 1986.71 | 1996.38 | 1989.54 | 2.83 | 6.83 | 9.67 | 158.50 | 12.30 | 4.67 | 184.90 | 26.40 |
| 23 | 1996.38 | 2008.88 | 2000.29 | 3.92 | 8.58 | 12.50 | 120.80 | 8.00 | 3.89 | 118.82 | 1.98 |
| 24 | 2008.88 | – | 2014.29 | 5.42 | – | – | 81.90 | 1.70 | **3.10** | 85.15 | 3.25 |

value of the sunspot number on the $j$th day. It should be noted that estimates of $\Delta S$ are sensitive to the choice of the length of the smoothing window ($L$) used in Equation (1). A larger or smaller window size can smooth the data too much or too little. Therefore adequate caution should be exercised while choosing a smoothing window in order to draw statistically meaningful information on inherent variation present in the daily sunspot number. This point was taken into account in an earlier study by Kakad, Kakad, and Ramesh (2015) using different smoothing windows on daily sunspot numbers. Their study suggested that a smoothing window of nine days is reasonable to retrieve a meaningful value for $\Delta S$, therefore we take $L = 9$ days in this study. The estimated $\Delta S$ is treated as a random variable to compute the Shannon entropy, and it is given by

$$E = -\sum_{l=1}^{l=m} p(y_l) \log_2\big[p(y_l)\big], \tag{2}$$

where $y$ is a random variable with $m$ the number of outcomes, and $p(y_l)$ is the probability of $y_l$. It is clear from Equation (2) that one requires information on the probability distribution function of the random variable $y_l$ in order to estimate the Shannon entropy. We obtained the probability distribution function using the histogram technique (Wallis, 2006). The Shannon entropy can now be obtained using

$$E = -\sum_{k=1}^{k=N} p_k \log_2(p_k) + \log_2(w_k), \tag{3}$$

where $p_k$ is the probability, $w_k$ is the width of the $k$th bin of the histogram, and $N$ is the total number of bins in the histogram. The estimated probability density function is such that $\sum_{k=1}^{k=N} p_k = 1$. We determine the bin width using Scott's method, where $w_k = 3.49\sigma/m^{1/3}$ (Scott, 1979). Here $\sigma$ and $m$ indicate the standard deviation in $\Delta S$ and the number of random observations, respectively.

It may be noted that Kakad, Kakad, and Ramesh (2015) computed the entropy associated with each SC, and it was found to vary with the SC number. It is well documented that solar activity changes within a SC. For example, the rate at which it increases in the ascending phase or decreases in the descending phase are not same. The duration of the ascending and descending phases is not the same either. It is known that SC 23 had an extended minimum that resulted in a longer descending time for that SC. Although not yet verified, it is possible that the association of a variable degree of randomness with these different phases of SCs could be one reason for the above observation. Thus, we examine the entropy related to different phases of a given SC. For this purpose, we divide each SC into five parts of equal length. These partitions are illustrated in Figure 1 superposed with the daily (red) and monthly averaged (blue) sunspot number of SC 21. Here each part of the $n$th SC has a length of $T_{\rm cy}^n/5$, and we treat them as different phases of the SC, starting from Phase 1 (P1) to Phase 5 (P5). Phase 1 (P1) of the $n$th SC starts at $t_{\rm s}^n$ and ends at $t_{\rm s}^n + T_{\rm cy}^n/5$. Consequently, Phase 5 (P5) of the $n$th SC starts at $t_{\rm e}^n - T_{\rm cy}^n/5$ and ends at $t_{\rm e}^n$.

As an example, the $\Delta S$ (upper panels) and corresponding probability distribution function (lower panels) during P5 for (a) SC 21 and (b) SC 22 are shown in Figure 2. This figure indicates that the shapes of the probability distribution function during the ending phase of SC 21 and SC 22 are different, and the corresponding entropy values are 4.59 and 4.67, respectively. For each SC, we have five entropy values corresponding to P1 to P5. We have displayed the time variation of the entropy in the different phases of an SC in Figure 3a for SC 10 – 24. The vertical black dashed-dotted line and red dotted line indicate the time of the start ($t_{\rm s}^n$) and peak ($t_{\rm p}^n$) for each SC, respectively. It is clearly evident that the entropy does

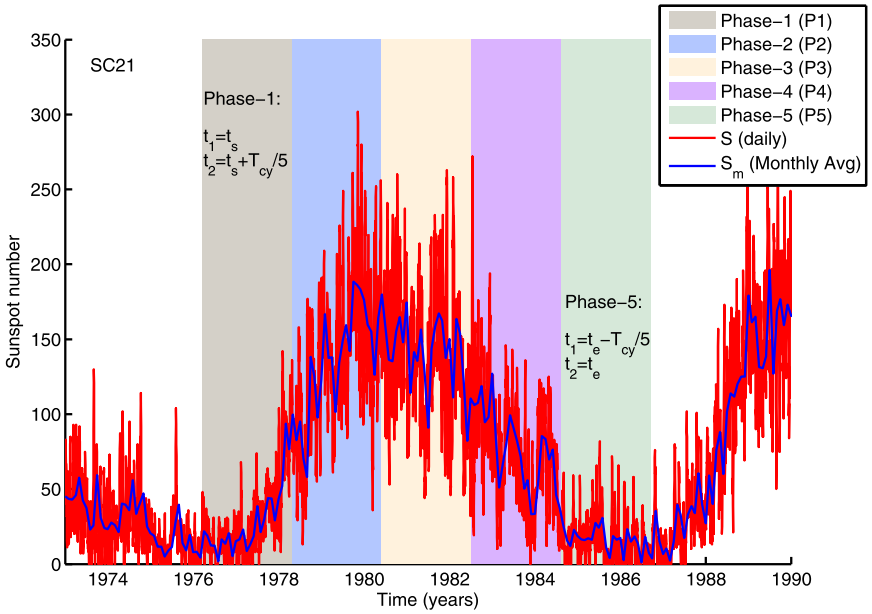


**Figure 1** Variation of daily (red) and monthly average (blue) sunspot numbers are shown for SC 21. The SC is divided in to five parts of equal length (*i.e.* $T_{cy}^{21}/5$) as marked by vertical column of different colors. Each part is considered as one phase and they are respectively termed as Phase 1 to Phase 5.

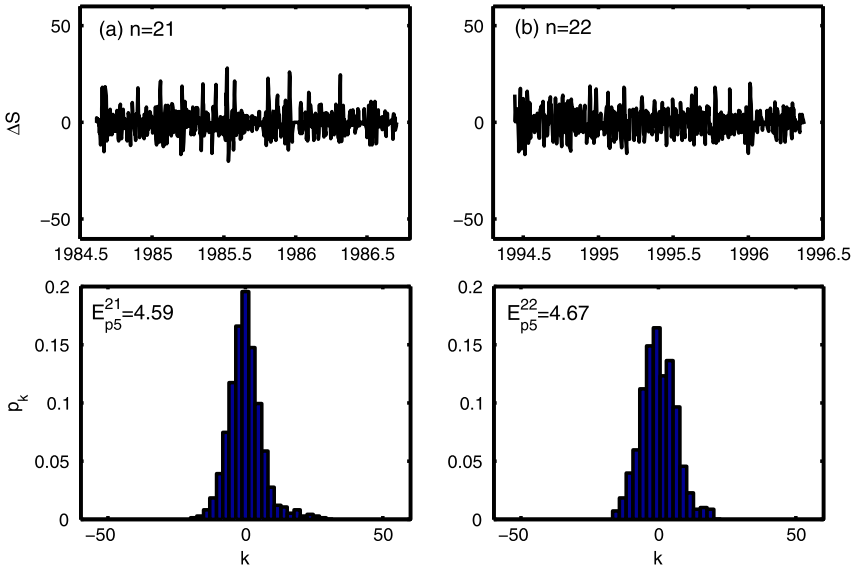


**Figure 2** Variations in daily sunspot numbers ($\Delta S$) are shown in the upper panel with their corresponding probability distribution function in the lower panel for Phase-5 of (a) SC 21 and (b) SC 22. The entropy values during P5 are mentioned in the corresponding subplot.

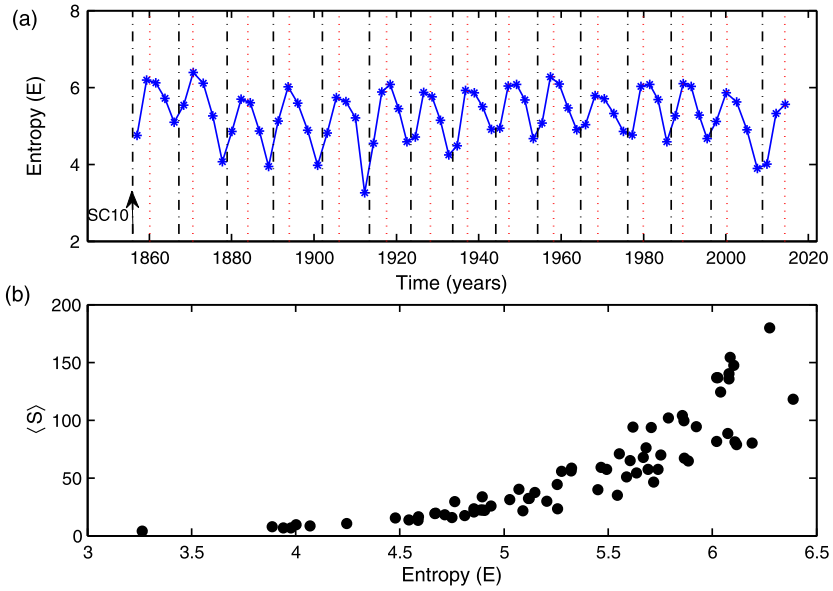


**Figure 3** (a) Variation of entropy during different phases for SCs 10 – 24 are shown as a function of time. Each filled dot represents the entropy value during one of the phases corresponding to P1 to P5. (b) The average sunspot number during each phase is plotted with its corresponding value of entropy for SCs 10 – 24. It is found that the higher (lower) values of entropy are associated with maximum (minimum) average sunspot number.

change with the phase of solar activity. In Figure 3b we show the plot of the average sunspot number ($\langle S \rangle$) during different phases as a function of corresponding entropy values for each solar cycle (SCs 10 – 24). Thus, it is clearly evident that the distinct phases (P1 – P5) of the solar cycle yield varied entropy values. Lower (higher) entropy values are associated with periods of lower (higher) sunspot numbers.

## 3. Results and Discussion

With the understanding that the degree of randomness varies with the phases of an SC, we prefer to use this information in developing a prediction scheme for estimating the peak smoothed sunspot number. In other words, our aim is to forecast the peak SSN for the $(n+1)$th SC using the available information of the preceding SCs in terms of entropy, ascent time, descent time, length, *etc*. In particular, we proceed to test whether the entropy information in different phases of past SCs can be employed to predict the peak SSN of the $(n+1)$th SC. In order to develop such a prediction model, the dependence of the peak SSN of the $(n+1)$th SC on the entropy values in different phases of the preceding four SCs, *i.e.* cycles $n$, $n-1$, $n-2$, and $n-3$, is examined. In this preliminary analysis, it is noted that $S_{\max}^{n+1}$ correlates well with two parameters, namely i) the entropy during phase P5 of SC $n$, and ii) the descent time of the SC $n-2$. This yields correlation coefficients of 0.60 and 0.76, respectively. When these two parameters are combined in the form $E_{\mathrm{P5}}^{n}/T_{\mathrm{d}}^{n-2}$, the correlation significantly improves to 0.87. Thus, $E_{\mathrm{P5}}^{n}/T_{\mathrm{d}}^{n-2}$ is designated as parameter $X$ and used further in the development of the forecasting model. Several tests reveal that when a dimensionless quantity $[T_{\mathrm{a}}^{n-3}/T_{\mathrm{cy}}^{n-1}]$ is used to scale $S_{\max}^{n+1}$, this correlation improves

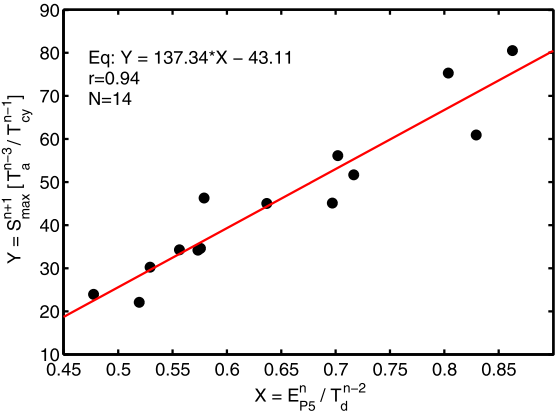


**Figure 4** We define two parameters ($X = E^n_{P5}/T^{n-2}_d$ and $Y = S^{n+1}_{max}[T^{n-3}_a/T^{n-1}_{cy}]$) for the model. $Y$ is plotted as a function of $X$. The correlation coefficient is 0.94 and it is based on the entropy estimates for SCs 10 – 23 *i.e.* $N = 14$. The linear least-square fit equation is shown in the plot.

substantially to 0.94. Therefore, we define $S^{n+1}_{max}[T^{n-3}_a/T^{n-1}_{cy}]$ as our parameter $Y$ and use it in the forecast model development.

Based on the above analysis, it is found that of the different phases, entropy values corresponding to P5 of SC $n$ (*i.e.* $E^n_{P5}$) best predict the peak SSN of SC $n+1$. In addition to the entropy estimates of P5 of the $n$th SC, we use the ascent time, descent time, and length of the preceding SCs in the present prediction model. The model parameters are $X = E^n_{P5}/T^{n-2}_d$ and $Y = S^{n+1}_{max}[T^{n-3}_a/T^{n-1}_{cy}]$. Figure 4 depicts the relation between parameter $Y$ and $X$ for SCs 10 – 23. It shows a strong dependence between these parameters, with a correlation coefficient of $r = 0.94$. Thus the correlation coefficient is based on $N = 14$ data points and is statistically above the 99% significance level. The obtained linear fit between $X$ and $Y$ gives rise to the following regression:

$$S^{n+1}_{max}\left[\frac{T^{n-3}_a}{T^{n-1}_{cy}}\right] = 137.34\left[\frac{E^n_{P5}}{T^{n-2}_d}\right] - 43.11. \tag{4}$$

This equation indicates that the forecast for the peak SSN of SC $n+1$ becomes possible when the entropy toward the end of the preceding SC (SC $n$), *i.e.* during P5, is available. We used this prediction equation to obtain the peak SSNs for SCs 10 – 23, and these estimates are compared with the observed peak SSN of the corresponding SCs. Figure 5a illustrates the comparison of observed (red) and predicted (black) peak SSNs for SCs 10 – 23. The peak SSN predictions for the past SCs *i.e.* $n = 11-24$ are in general agreement with the observed peak SSNs for the corresponding SCs. The absolute difference between the predicted and observed peak SSNs is given in the last column of Table 1. Overall, the difference in observed and predicted peak SSN values lies in the range of 1 – 26, with an average value $\langle\zeta_{error}\rangle = 11.3$. The absolute errors for SCs 12, 17, 18, and 22 are relatively high ($\zeta_{error} > 20$) compared to other SCs.

With the present prediction model, the forecast of the peak SSN for the immediately following SC is possible only after the end of the preceding SC. Our aim is to enable forecasting of the peak SSN for SC 25. Keeping this in view, we plot the entropy during P5 for SCs 10 – 23 as shown in Figure 5b. It may be noted that SC 24 is in its declining phase and has not yet ceased. As the entropy value of P5 related to SC 24 is not available yet, the forecast of the peak SSN of SC 25 using Equation (4) is not feasible. However, we attempt to circumvent this situation using information available for SCs 22 and 23 as follows. If we assume that the obtained decreasing entropy trend of P5 (from 4.66 to 3.89) related to SC 22 and SC 23 is to continue at the same rate during SC 24, then the entropy of P5 for SC 24

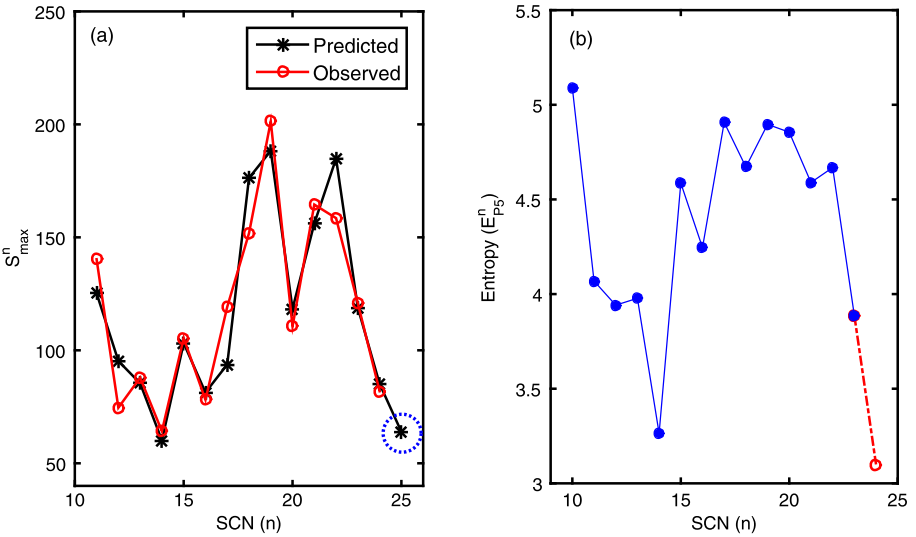


**Figure 5** (a) Observed (red) and predicted peak smoothed sunspot number for SCs 10 – 24. It suggests that the observed and predicted SSN are in good agreement and the average absolute error in the predicted SSN is 11.3. The forecast of peak SSN for SC 25 of $S^{25}_{\max} = 63 \pm 11.3$ is marked by a circle. (b) Shannon Entropy during the ending phase of each SC (*i.e.* Phase 5) as a function of SC number for SCs 10 – 23. The value of entropy is approximated for SC 24 using the trend of entropy from SC 22 – 23. This approximate estimate of $E^{24}_{\rm P5} = 3.1$ is shown by the red circles.

is 3.1. This is shown as the red circle in Figure 5b and is also mentioned in Table 1. By considering this derived entropy value to be correct, the proposed prediction equation yields an estimate of 63±11.3 as the peak SSN of SC 25. This predicted value of $S^{25}_{\max}$ is marked as a dotted circle in Figure 5a. Several other studies provided peak SSN values in the range 63 to 100 from different approaches. While a study by Hathaway and Wilson (2004) suggested a peak SSN of 70±30, Janardhan *et al.* (2015) used photospheric magnetic field data and provided an estimate of 62±12 for the peak SSN of SC 25. In addition to these, there were other studies that suggested that the peak SSN of SC 25 would be greater than 100 (Tripathy, 2016).

A careful examination of Equation (4) indicates that the peak SSN of a forthcoming SC is dependent on the degree of randomness present during the ending phase of the preceding SC. If the right-hand side of Equation (4) becomes smaller than zero, then mathematically it will give negative values for the peak sunspot number, which is a nonphysical situation. Thus, one can find the critical entropy value that is required to maintain the positive peak sunspot number by equating the right-hand side of Equation (4) to zero. It should be noted that the descent time term $T_{\rm d}^{n-2}$ that appears on the right side of Equation (4) varies from one SC to another. While computing the critical entropy, we use the average estimate of the descent time for SCs 1 – 23, which is $\langle T_{\rm d} \rangle = 6.75 \pm 1.33$ years. Adopting this simple procedure, we obtain the critical entropy for P5 as $E^C_{\rm P5} = 43.11 \langle T_{\rm d} \rangle / 137.34$. These calculations suggest that if the entropy value during P5 of the preceding SC falls below a critical limit of 1.7±0.40, then the following solar activity can enter into a physically non-realizable situation that cannot be explained using the proposed prediction equation.

## 4. Conclusions

In the present study a new model was developed to predict the peak smoothed sunspot of a forthcoming SC. This model uses estimates of the Shannon entropy, a measure of inherent randomness, in the ending phase of a preceding SC termed Phase 5. In addition to this, the ascent time, descent time, and length of the preceding SCs are also used in the model. The prediction model is represented by Equation (4) in the previous section. This model prediction equation is based on the entropy estimates for SCs 10 – 23. The parameters $X = E_{\mathrm{P5}}^{n}/T_{\mathrm{d}}^{n-2}$ and $Y = S_{\max}^{n+1}[T_{\mathrm{a}}^{n-3}/T_{\mathrm{cy}}^{n-1}]$ defined for the models have a correlation coefficient of 0.94. The average absolute error in the predicted and observed SSN is found to be 11.3. It may be noted that the prediction using the proposed model is available at the start of a new SC. As SC 24 has not yet ceased, we derived the approximate entropy value for SC 24 based on the trend of entropy from SCs 22 – 23. By assuming the estimated entropy value of $E_{\mathrm{P5}}^{24} = 3.1$ to be correct, we predict the peak SSN for SC 25 to be 63±11.3. Although the prediction of the peak SSN for SC 25 is based on some approximations, it suggests weaker solar activity similar to the well-known Dalton minimum. In contrast, if the entropy value during P5 of SC 24 does not fall drastically, as speculated in Figure 5b, and remains closer to the corresponding entropy value of SC 23, then the prediction for SC 25 is 116±11.3. We also obtained the limiting or critical entropy value during the ending phase of the preceding SC, which is required to maintain a positive SSN for an upcoming SC. If the entropy during the ending phase of the $n$th SC falls below the critical value of $E_{\mathrm{P5}}^{C} = 1.7 \pm 0.4$, then the following solar activity cannot be sustained to yield a positive SSN. A few other recent studies have suggested a weaker activity for SC 25. Notably, Zachilas and Gkana (2015) concluded that the next 90 years are likely to witness a significant reduction in solar activity resembling the Maunder minimum. These authors have also tested their neural network-based model that incorporates the newly revised sunspot number series (Version 2) and arrived at the same conclusions as above that the upcoming solar activity is indeed going to be low (Gkana and Zachilas, 2016).

**Acknowledgements** We thank the SIDC, SILSO team for the daily international sunspot data. This work is carried out under the Project ITAG-EMG(GV) of IIG, India.

**Disclosure of Potential Conflicts of Interest** The authors declare that they have no conflicts of interest.

## References

Bapanayya, C., Raju, P., Sharma, S.D., Ramesh, D.: 2011, Information theory-based measures of similarity for imaging shallow-mantle discontinuities. *Lithosphere* **3**(4), 289. DOI.

Carbone, A., Castelli, G., Stanley, H.: 2004, Analysis of clusters formed by the moving average of a long-range correlated time series. *Phys. Rev. E* **69**(2), 026105. DOI.

Clilverd, M.A., Clarke, E., Ulich, T., Rishbeth, H., Jarvis, M.J.: 2006, Predicting solar cycle 24 and beyond. *Space Weather* **4**(9), S09005. DOI.

Das Sharma, S., Ramesh, D., Bapanayya, C., Raju, P.: 2012, Sea surface temperatures in cooler climate stages bear more similarity with atmospheric $CO_2$ forcing. *J. Geophys. Res., Atmos.* **117**(D13), D13110. DOI.

De Michelis, P., Consolini, G., Materassi, M., Tozzi, R.: 2011, An information theory approach to the storm-substorm relationship. *J. Geophys. Res. Space Phys.* **116**(A8), A08225. DOI.

de Toma, G., Gibson, S., Emery, B., Arge, C.: 2010, The minimum between cycle 23 and 24: Is sunspot number the whole story? In: *SOHO-23: Understanding a Peculiar Solar Minimum* **428**, 217. ADS.

Dikpati, M., Charbonneau, P.: 1999, A Babcock–Leighton flux transport dynamo with solar-like differential rotation. *Astrophys. J.* **518**(1), 508. DOI.

Dikpati, M., Gilman, P.A.: 2008, Global solar dynamo models: Simulations and predictions. *J. Astrophys. Astron.* **29**(1 – 2), 29. DOI.

Dikpati, M., De Toma, G., Gilman, P.A.: 2006, Predicting the strength of solar cycle 24 using a flux-transport dynamo-based tool. *Geophys. Res. Lett.* **33**(5), L05102. DOI.
Emmert, J., Lean, J., Picone, J.: 2010, Record-low thermospheric density during the 2008 solar minimum. *Geophys. Res. Lett.* **37**(12), L12102. DOI.
Ermolli, I., Matthes, K., Dudok de Wit, T., Krivova, N.A., Tourpali, K., Weber, M., Unruh, Y.C., Gray, L., Langematz, U., Pilewskie, P., *et al.*: 2013, Recent variability of the solar spectral irradiance and its impact on climate modelling. *Atmos. Chem. Phys.* **13**(8), 3945. DOI.
Feynman, J.: 1982, Geomagnetic and solar wind cycles, 1900 – 1975. *J. Geophys. Res. Space Phys.* **87**(A8), 6153. DOI.
Gkana, A., Zachilas, L.: 2015, Sunspot numbers: Data analysis, predictions and economic impacts. *J. Eng. Sci. Tech. Rev.* **8**, 79. http://www.jestr.org/downloads/Volume8Issue1/fulltext148115.pdf.
Gkana, A., Zachilas, L.: 2016, Re-evaluation of predictive models in light of new data: Sunspot number version 2.0. *Solar Phys.* **291**, 2457. DOI.
Hajra, R., Tsurutani, B.T., Echer, E., Gonzalez, W.D.: 2014, Relativistic electron acceleration during high-intensity, long-duration, continuous AE activity (HILDCAA) events: Solar cycle phase dependences. *Geophys. Res. Lett.* **41**(6), 1876. DOI.
Hao, Y., Shi, H., Xiao, Z., Zhang, D.: 2014, Weak ionization of the global ionosphere in solar cycle 24. In: *Annales Geophysicae* **32**, 809. Copernicus GmbH. DOI.
Hathaway, D.H.: 2010, The solar cycle. *Living Rev. Solar Phys.* **7**(1), 1. DOI.
Hathaway, D.H., Wilson, R.M.: 2004, What the sunspot record tells us about space climate. *Solar Phys.* **224**(1 – 2), 5. DOI.
Hathaway, D.H., Wilson, R.M.: 2006, Geomagnetic activity indicates large amplitude for sunspot cycle 24. *Geophys. Res. Lett.* **33**(18), L18101. DOI.
Janardhan, P., Bisoi, S.K., Ananthakrishnan, S., Tokumaru, M., Fujiki, K., Jose, L., Sridharan, R.: 2015, A 20 year decline in solar photospheric magnetic fields: Inner-heliospheric signatures and possible implications. *J. Geophys. Res. Space Phys.* **120**(7), 5306. DOI.
Kakad, B.: 2011, A new method for prediction of peak sunspot number and ascent time of the solar cycle. *Solar Phys.* **270**(1), 393. DOI.
Kakad, B., Kakad, A., Ramesh, D.S.: 2015, A new method for forecasting the solar cycle descent time. *J. Space Weather Space Clim.* **5**, A29. DOI.
Kane, R.: 2007, A preliminary estimate of the size of the coming solar cycle 24, based on Ohl's precursor method. *Solar Phys.* **243**(2), 205. DOI.
Materassi, M., Wernik, A., Yordanova, E.: 2007, Determining the verse of magnetic turbulent cascades in the Earth's magnetospheric cusp via transfer entropy analysis: Preliminary results. *Nonlinear Process. Geophys.* **14**(2), 153. DOI.
McComas, D., Ebert, R., Elliott, H., Goldstein, B., Gosling, J., Schwadron, N., Skoug, R.: 2008, Weaker solar wind from the polar coronal holes and the whole Sun. *Geophys. Res. Lett.* **35**(18), L18103. DOI.
Mundt, M.D., Maguire, W.B., Chase, R.R.P.: 1991, Chaos in the sunspot cycle: Analysis and prediction. *J. Geophys. Res. Space Phys.* **96**(A2), 1705. DOI.
Muñoz-Jaramillo, A., Dasi-Espuig, M., Balmaceda, L.A., DeLuca, E.E.: 2013, Solar cycle propagation, memory, and prediction: Insights from a century of magnetic proxies. *Astrophys. J. Lett.* **767**(2), L25. DOI.
Ohl, A.: 1966, Wolf's number prediction for the maximum of the cycle 20. *Soln. Dannye* **12**, 84.
Pesnell, W.D.: 2008, Predictions of solar cycle 24. *Solar Phys.* **252**(1), 209. DOI.
Pesnell, W.D.: 2014, Predicting solar cycle 24 using a geomagnetic precursor pair. *Solar Phys.* **289**(6), 2317. DOI.
Pesnell, W.D.: 2016, Predictions of solar cycle 24: How are we doing? *Space Weather* **14**(1), 10. DOI.
Pishkalo, M.I.: 2014, Prediction of solar cycle 24 using sunspot number near the cycle minimum. *Solar Phys.* **289**(5), 1815. DOI.
Price, C.P., Prichard, D., Hogenson, E.A.: 1992, Do the sunspot numbers form a "chaotic" set? *J. Geophys. Res. Space Phys.* **97**(A12), 19113. DOI.
Scott, D.W.: 1979, On optimal and data-based histograms. *Biometrika* **66**, 605. http://www.jstor.org/stable/2335182.
Shannon, C.E.: 1948, A mathematical theory of communication. *Bell Syst. Tech. J.* **27**, 379.
Solomon, S.C., Qian, L., Burns, A.G.: 2013, The anomalous ionosphere between solar cycles 23 and 24. *J. Geophys. Res. Space Phys.* **118**(10), 6524. DOI.
Svalgaard, L., Kamide, Y.: 2012, Asymmetric solar polar field reversals. *Astrophys. J.* **763**(1), 23. DOI.
Svalgaard, L., Cliver, E.W., Kamide, Y.: 2005, Sunspot cycle 24: Smallest cycle in 100 years? *Geophys. Res. Lett.* **32**(1), L01104. DOI.
Thompson, R.: 1993, A technique for predicting the amplitude of the solar cycle. *Solar Phys.* **148**(2), 383. DOI.
Tripathy, S.C.: 2016, Predictions of solar cycle. *Asian J. Phys.* **25**, 387. ADS.

Usoskin, I.G., Solanki, S., Kovaltsov, G.: 2007, Grand minima and maxima of solar activity: New observational constraints. *Astron. Astrophys.* **471**(1), 301. DOI.

Usoskin, I.G., Solanki, S., Kovaltsov, G.: 2011, Grand minima of solar activity during the last millennia. *Proc. Int. Astron. Union* **7**(S286), 372. DOI.

Vichare, G., Bhaskar, A., Ramesh, D.S.: 2016, Are the equatorial electrojet and the Sq coupled systems? transfer entropy approach. *Adv. Space Res.* **57**(9), 1859. DOI.

Wallis, K.: 2006, A note on the calculation of entropy from histograms.

Wilson, R.M.: 1990, On the level of skill in predicting maximum sunspot number: A comparative study of single variate and bivariate precursor techniques. *Solar Phys.* **125**(1), 143. DOI.

Zachilas, L., Gkana, A.: 2015, On the verge of a grand solar minimum: A second Maunder minimum? *Solar Phys.* **290**(5), 1457. DOI.

Zhao, L.-L., Qin, G.: 2013, An observation-based GCR model of heavy nuclei: Measurements from CRIS onboard ACE spacecraft. *J. Geophys. Res. Space Phys.* **118**(5), 1837. DOI.